AIAA 2011-3043

20th AIAA Computational Fluid Dynamics Conference, 27 - 30 June, Honolulu, Hawaii, 2011

New-Generation Hyperbolic Navier-Stokes Schemes: $O(1/h)$ Speed-Up and Accurate Viscous/Heat Fluxes

Hiroaki Nishikawa*

National Institute of Aerospace, Hampton, VA 23666, USA

In this paper, we introduce a first-order hyperbolic system model for viscous flows, and propose a unique way of computing steady viscous flows: integrate the hyperbolic Navier-Stokes system in time toward the steady state. We construct an upwind finite-volume scheme for the hyperbolic Navier-Stokes system and demonstrate remarkable advantages of the resulting Navier-Stokes code: $O(1/h)$ speed-up over traditional Navier-Stokes codes, where h is the mesh spacing, and the capability of simultaneously computing the viscous stresses and the heat fluxes to the same order of accuracy as that of the main variables on irregular grids. The paper concludes with discussions on the future developments and the potential impact on the future algorithm development for computational fluid dynamics.

1. Introduction

In this paper, we extend the first-order hyperbolic system method developed for model equations in a series of papers [1,2] to the Navier-Stokes equations. We thereby propose a non-traditional way of computing viscous flows: integrate an equivalent first-order hyperbolic system in time toward the steady state. The first-order system is deliberately designed such that it reduces to the original Navier-Stokes equations in the steady state; its viscous part is a *hyperbolic* system on its own. Navier-Stokes codes arising from the proposed method will be radically different from those currently used.

Simplified Discretization

Robust and accurate viscous discretization is made simple because the viscous term is hyperbolic just like the inviscid term. Methods developed for the inviscid term such as upwind fluxes and limiters, are directly applied to the viscous term. The first-order hyperbolic system method has a great potential for overcoming many difficulties associated with the viscous discretization encountered particularly in unstructured grids and high-order methods (see [3,4] and references therein). Note that the proposed method is different from the mixed finite-element method [5] and other first-order system methods [6,7] in that our system is *hyperbolic in time* while their systems have no such characterization. It is the hyperbolicity that brings a drastic change in the viscous discretization.

$O(1/h)$ Speed-up

Because the system is hyperbolic, the explicit time step is determined by the CFL condition, leading to an $O(h)$ time step where h is the mesh spacing. It implies $O(1/h)$ speed-up over traditional schemes with an $O(h^2)$ time step. For implicit time-stepping schemes, the advantage comes in the condition number of the linearized system to be inverted at every time step: $O(1/h)$ versus $O(1/h^2)$. It brings $O(1/h)$ speed-up for iterative methods for solving the linearized system. In either case, the acceleration factor grows for larger-scale problems. In three-dimensional simulations, it will be $O(100)$ for 1 million grid points, and $O(1000)$ for 1 billion grid points. Such an orders-of-magnitude improvement in the algorithm will not only allow us to overcome the current hardware limit, but also bring a continuously-growing advantage for larger-scale problems along with the increase in computing power.

*Senior Research Scientist (hiro@nianet.org), National Institute of Aerospace, 100 Exploration Way, Hampton, VA 23666 USA

Accurate Viscous/Heat Fluxes

The first-order hyperbolic system method generates a new class of Navier-Stokes codes that are capable of computing the viscous stresses and the heat fluxes simultaneously with the main flow variables to the same order of accuracy on irregular grids. The use of irregular grids is common in practical applications due to complex geometries; the irregularity is hard to avoid particularly once we start adapting grids for viscous flows. On such grids, the physical quantities sought by the viscous simulation, such as the viscous stresses and the heat fluxes, can be obtained only with a lower order of accuracy, typically one order less than that of the main flow variables. They also often exhibit erroneous behavior. For example, current state-of-the-art Navier-Stokes codes are known to produce erratic viscous stress and heating distributions [8, 9]. The proposed method has a great potential for overcoming these difficulties. Also, it can be extended to produce accurate vorticity as well as the viscous stresses and the heat fluxes.

The core of the proposed method lies in the construction of a hyperbolic model for viscous flows. Therefore, *it is fully compatible with virtually any numerical method* (e.g., finite-volume/element, residual-distribution, and other modern higher-order methods such as discontinuous Galerkin and spectral-volume/difference methods). Many advantages such as those described above are *intrinsic properties* of the proposed method. In this paper, we present an example of such a hyperbolic model for the compressible Navier-Stokes equations, and show how it can be discretized by the finite-volume method. We present preliminary results obtained by the resulting Navier-Stokes code, and demonstrate the $O(1/h)$ speed-up and accurate viscous/heat fluxes on irregular grids. Finally, we discuss the future developments and the impact of the proposed method on the future algorithm development in computational fluid dynamics (CFD).

2. First-Order Hyperbolic Navier-Stokes System

2.1. One Dimension

Consider the compressible Navier-Stokes equations in one dimension:

$$\frac{\partial \rho}{\partial t} + \frac{\partial (\rho u)}{\partial x} = 0, \tag{2.1}$$

$$\frac{\partial (\rho u)}{\partial t} + \frac{\partial (\rho u^2 + p - \tau)}{\partial x} = 0, \tag{2.2}$$

$$\frac{\partial (\rho E)}{\partial t} + \frac{\partial (\rho u H - \tau u + q)}{\partial x} = 0, \tag{2.3}$$

where ρ is the density, u is the velocity, p is the pressure, E is the specific total energy, and $H = E + p/\rho$ is the specific total enthalpy. The viscous stress τ and the heat flux q are given by

$$\tau = \frac{4}{3}\mu \frac{\partial u}{\partial x}, \quad q = -\frac{\mu}{Pr(\gamma - 1)} \frac{\partial T}{\partial x}, \tag{2.4}$$

where T is the temperature, γ is the ratio of specific heats, Pr is the Prandtl number, μ is the viscosity defined by Sutherland's law, and Stokes' hypothesis has been assumed. All the quantities are assumed to be nondimensionalized by their free stream values except that the velocity and the pressure are scaled by the speed of sound a_∞ and the dynamic pressure $\rho_\infty a_\infty^2$, respectively. Thus, the viscosity is given by the following form of Sutherland's law:

$$\mu = \frac{M_\infty}{Re_\infty} \frac{1 + C/T_\infty}{T + C/T_\infty} T^{\frac{3}{2}}, \tag{2.5}$$

where T_∞ is the dimensional free stream temperature, and $C = 110.5$ [K] is the Sutherland constant. The ratio of the free stream Mach number, M_∞, to the free stream Reynolds number, Re_∞, arise from the nondimensionalization. The system is closed by the nondimensionalized equation of state for ideal gases:

$$\gamma p = \rho T. \tag{2.6}$$

Traditionally, the Navier-Stokes system is discretized in two steps: the inviscid term is discretized by a method suitable for hyperbolic systems (e.g., upwind differencing) followed by the discretization of the viscous term by a method suitable for parabolic equations (e.g., central differencing). We challenge the tradition by proposing the following first-order system model:

$$\frac{\partial \rho}{\partial t} + \frac{\partial(\rho u)}{\partial x} = 0, \tag{2.7}$$

$$\frac{\partial(\rho u)}{\partial t} + \frac{\partial(\rho u^2 + p - \tau)}{\partial x} = 0, \tag{2.8}$$

$$\frac{\partial(\rho E)}{\partial t} + \frac{\partial(\rho u H - \tau u + q)}{\partial x} = 0, \tag{2.9}$$

$$\frac{\partial \tau}{\partial t} - \frac{\mu_v}{T_v}\left(\frac{\partial u}{\partial x} - \frac{\tau}{\mu_v}\right) = 0, \tag{2.10}$$

$$\frac{\partial q}{\partial t} - \frac{\mu_h}{T_h}\left(-\frac{1}{\gamma(\gamma-1)}\frac{\partial T}{\partial x} - \frac{q}{\mu_h}\right) = 0, \tag{2.11}$$

where μ_v and μ_h are the scaled viscosities,

$$\mu_v = \frac{4}{3}\mu, \quad \mu_h = \frac{\gamma\mu}{Pr}, \tag{2.12}$$

T_v and T_h are relaxation times associated with the viscous stress and the heat flux. Note that the first-order system has been deliberately constructed such that it reduces to the original Navier-Stokes system in the steady state for *arbitrary* T_v and T_h. Based on the previous work [1, 2], we define these relaxation times as

$$T_v = \frac{L^2}{\nu_v}, \quad T_h = \frac{L^2}{\nu_h}, \tag{2.13}$$

where L is a length scale of $O(1)$ defined as suggested in Ref. [2], and ν_v and ν_h are the kinematic viscosities,

$$\nu_v = \frac{\mu_v}{\rho}, \quad \nu_h = \frac{\mu_h}{\rho}. \tag{2.14}$$

As we will see shortly, the viscous term of the first-order system is hyperbolic, and therefore the whole system can be discretized by a method for hyperbolic systems only. The first-order system is then integrated in time to the steady state; the steady solution, including the viscous stress and the heat flux, will satisfy the original Navier-Stokes equations. Accuracy of the solution is determined by the discretization method, and it is expected to be uniform for all variables. For simple and systematic discretization, we cast the first-order system in the following preconditioned conservative form:

$$\mathbf{P}^{-1}\frac{\partial \mathbf{U}}{\partial t} + \frac{\partial \mathbf{F}}{\partial x} = \mathbf{S}, \tag{2.15}$$

where

$$\mathbf{U} = \begin{bmatrix} \rho \\ \rho u \\ \rho E \\ \tau \\ q \end{bmatrix}, \quad \mathbf{F} = \begin{bmatrix} \rho u \\ \rho u^2 + p - \tau \\ \rho u H - \tau u + q \\ -u \\ \dfrac{a^2}{\gamma(\gamma-1)} \end{bmatrix}, \quad \mathbf{S} = \begin{bmatrix} 0 \\ 0 \\ 0 \\ \tau/\mu_v \\ q/\mu_h \end{bmatrix}, \quad \mathbf{P}^{-1} = \begin{bmatrix} 1 & 0 & 0 & 0 & 0 \\ 0 & 1 & 0 & 0 & 0 \\ 0 & 0 & 1 & 0 & 0 \\ 0 & 0 & 0 & T_v/\mu_v & 0 \\ 0 & 0 & 0 & 0 & T_h/\mu_h \end{bmatrix}, \tag{2.16}$$

where $a = \sqrt{\gamma p/\rho} = \sqrt{T}$ is the speed of sound. The matrix $\mathbf{P}$ can be thought of as a local-preconditioning matrix. The wave structure of the system can be analyzed, in principle, by the Jacobian matrix:

$$\mathbf{PA} = \mathbf{P}\frac{\partial \mathbf{F}}{\partial \mathbf{U}}, \tag{2.17}$$

but it has not been fully analyzed yet. Meanwhile, we split the Jacobian into the inviscid and viscous parts:

$$\mathbf{PA} = \mathbf{PA^i} + \mathbf{PA^v}, \tag{2.18}$$

where $\mathbf{A^i}$ and $\mathbf{A^v}$ are the Jacobians derived from the inviscid and viscous fluxes, respectively:

$$\mathbf{F^i} = \begin{bmatrix} \rho u \\ \rho u^2 + p \\ \rho u H \\ 0 \\ 0 \end{bmatrix}, \quad \mathbf{F^v} = \begin{bmatrix} 0 \\ -\tau \\ -\tau u + q \\ -u \\ \dfrac{a^2}{\gamma(\gamma-1)} \end{bmatrix}. \tag{2.19}$$

The eigen-structure of the inviscid Jacobian is well known: the eigenvalues are

$$\lambda_1^i = u - a, \quad \lambda_2^i = u, \quad \lambda_3^i = u + a, \quad \lambda_{4,5}^i = 0, \tag{2.20}$$

with the corresponding linearly independent right-eigenvectors denoted by $\mathbf{r}_1^i$, $\mathbf{r}_2^i$, $\mathbf{r}_3^i$, $\mathbf{r}_4^i$, and $\mathbf{r}_5^i$. These eigenvectors represent the inviscid acoustic and entropy waves, constituting the inviscid subspaces. On the other hand, the viscous Jacobian has the following eigenvalues,

$$\lambda_1^v = -a_v, \quad \lambda_2^v = a_v, \quad \lambda_3^v = -a_h, \quad \lambda_4^v = a_h, \quad \lambda_5^v = 0, \tag{2.21}$$

where a_v and a_h are the viscous and heating wave speeds defined by

$$a_v = \sqrt{\frac{\nu_v}{T_v}}, \quad a_h = \sqrt{\frac{\nu_h}{T_h}}. \tag{2.22}$$

These eigenvalues imply that the viscous and heating waves are symmetric waves traveling in the opposite directions at the same speed. The associated right-eigenvectors are given by

$$\mathbf{r}_{1,2}^v = \begin{bmatrix} 0 \\ 1 \\ u \pm \dfrac{\tau Pr_n}{(Pr_n^2 - 1)\rho a_h} \\ \pm a_v \\ -\dfrac{\tau}{(Pr_n^2 - 1)\rho} \end{bmatrix}, \quad \mathbf{r}_{3,4}^v = \begin{bmatrix} 0 \\ 0 \\ 1 \\ 0 \\ \mp a_h \end{bmatrix}, \quad \mathbf{r}_5^v = \begin{bmatrix} 1 \\ u \\ E \\ 0 \\ 0 \end{bmatrix}, \tag{2.23}$$

where Pr_n is the ratio of the two wave speeds,

$$Pr_n \equiv \frac{a_v}{a_h}. \tag{2.24}$$

Clearly, these eigenvectors are linearly independent. It follows, therefore, that *the viscous part is a hyperbolic system by itself*, describing the symmetric viscous and heating waves.

In both the inviscid and viscous parts, the corresponding left-eigenvectors denoted by $\boldsymbol{\ell}_k^i$ and $\boldsymbol{\ell}_k^v$ where $k = 1, 5$ can be found since the right-eigenvectors are linearly independent. Then, the full Jacobian can be expressed as a sum of seven (not necessarily orthogonal) subspaces:

$$\mathbf{PA} = \sum_{k=1}^{3} \lambda_k^i \mathbf{\Pi}_k^i + \sum_{k=1}^{4} \lambda_k^v \mathbf{\Pi}_k^v, \tag{2.25}$$

where $\mathbf{\Pi}_k^i$ and $\mathbf{\Pi}_k^v$ are the pure inviscid and viscous projection matrices,

$$\mathbf{\Pi}_k^i = \mathbf{r}_k^i \boldsymbol{\ell}_k^i, \quad \mathbf{\Pi}_k^v = \mathbf{r}_k^v \boldsymbol{\ell}_k^v. \tag{2.26}$$

This is a sum of seven waves: three inviscid waves and two pairs of viscous and heating waves. The subspaces in each part are orthogonal to one another but not across the inviscid and viscous parts.

2.2. Two Dimensions

Consider the two-dimensional compressible Navier-Stokes equations:

$$\frac{\partial \rho}{\partial t} + \frac{\partial(\rho u)}{\partial x} + \frac{\partial(\rho v)}{\partial y} = 0, \tag{2.27}$$

$$\frac{\partial(\rho u)}{\partial t} + \frac{\partial(\rho u^2 + p - \tau_{xx})}{\partial x} + \frac{\partial(\rho uv - \tau_{yx})}{\partial y} = 0, \tag{2.28}$$

$$\frac{\partial(\rho v)}{\partial t} + \frac{\partial(\rho uv - \tau_{xy})}{\partial x} + \frac{\partial(\rho v^2 + p - \tau_{yy})}{\partial y} = 0, \tag{2.29}$$

$$\frac{\partial(\rho E)}{\partial t} + \frac{\partial(\rho uH - \tau_{xx}u - \tau_{xy}v + q_x)}{\partial x} + \frac{\partial(\rho vH - \tau_{yx}u - \tau_{yy}v + q_y)}{\partial x} = 0, \tag{2.30}$$

$$\tau_{xx} = \frac{2}{3}\mu\left(2\frac{\partial u}{\partial x} - \frac{\partial v}{\partial y}\right), \quad \tau_{xy} = \tau_{yx} = \mu\left(\frac{\partial u}{\partial y} + \frac{\partial v}{\partial x}\right), \quad \tau_{yy} = \frac{2}{3}\mu\left(2\frac{\partial v}{\partial y} - \frac{\partial u}{\partial x}\right), \tag{2.31}$$

$$q_x = -\frac{\mu}{Pr(\gamma-1)}\frac{\partial T}{\partial x}, \quad q_y = -\frac{\mu}{Pr(\gamma-1)}\frac{\partial T}{\partial y}, \tag{2.32}$$

where τ_{xx}, τ_{xy}, and τ_{yy} are the viscous stresses, and q_x and q_y are the heat fluxes. We construct a first-order Navier-Stokes system by replacing Equations (2.31) and (2.32) by the following evolution equations for the viscous stresses and the heat fluxes:

$$\frac{\partial \tau_{xx}}{\partial t} = \frac{\mu_v}{T_v}\left(\frac{\partial u}{\partial x} - \frac{1}{2}\frac{\partial v}{\partial y} - \frac{\tau_{xx}}{\mu_v}\right), \quad \frac{\partial \tau_{xy}}{\partial t} = \frac{\mu_v}{T_v}\left(\frac{3}{4}\frac{\partial u}{\partial y} + \frac{3}{4}\frac{\partial v}{\partial x} - \frac{\tau_{xy}}{\mu_v}\right), \frac{\partial \tau_{yy}}{\partial t} = \frac{\mu_v}{T_v}\left(\frac{\partial v}{\partial y} - \frac{1}{2}\frac{\partial u}{\partial x} - \frac{\tau_{yy}}{\mu_v}\right), \tag{2.33}$$

$$\frac{\partial q_x}{\partial t} = \frac{\mu_h}{T_h}\left(-\frac{1}{\gamma(\gamma-1)}\frac{\partial T}{\partial x} - \frac{q_x}{\mu_h}\right), \quad \frac{\partial q_y}{\partial t} = \frac{\mu_h}{T_h}\left(-\frac{1}{\gamma(\gamma-1)}\frac{\partial T}{\partial y} - \frac{q_y}{\mu_h}\right). \tag{2.34}$$

As in one dimension, we cast the first-order system in the form of a preconditioned conservative system:

$$\mathbf{P}^{-1}\frac{\partial \mathbf{U}}{\partial t} + \frac{\partial \mathbf{F}}{\partial x} + \frac{\partial \mathbf{G}}{\partial y} = \mathbf{S}, \tag{2.35}$$

where

$$\mathbf{U} = \begin{bmatrix} \rho \\ \rho u \\ \rho v \\ \rho E \\ \tau_{xx} \\ \tau_{xy} \\ \tau_{yy} \\ q_x \\ q_y \end{bmatrix}, \quad \mathbf{F} = \begin{bmatrix} \rho u \\ \rho u^2 + p - \tau_{xx} \\ \rho uv - \tau_{xy} \\ \rho uH - \tau_{xx}u - \tau_{xy}v + q_x \\ -u \\ -3v/4 \\ u/2 \\ \dfrac{a^2}{\gamma(\gamma-1)} \\ 0 \end{bmatrix}, \quad \mathbf{G} = \begin{bmatrix} \rho v \\ \rho uv - \tau_{xy} \\ \rho v^2 + p - \tau_{yy} \\ \rho vH - \tau_{xy}u - \tau_{yy}v + q_y \\ v/2 \\ -3u/4 \\ -v \\ 0 \\ \dfrac{a^2}{\gamma(\gamma-1)} \end{bmatrix}, \tag{2.36}$$

$$
\mathbf{S} = \begin{bmatrix} 0 \\ 0 \\ 0 \\ 0 \\ \tau_{xx}/\mu_v \\ \tau_{xy}/\mu_v \\ \tau_{yy}/\mu_v \\ q_x/\mu_h \\ q_y/\mu_h \end{bmatrix}, \quad \mathbf{P}^{-1} = \begin{bmatrix} 1 & 0 & 0 & 0 & 0 & 0 & 0 & 0 & 0 \\ 0 & 1 & 0 & 0 & 0 & 0 & 0 & 0 & 0 \\ 0 & 0 & 1 & 0 & 0 & 0 & 0 & 0 & 0 \\ 0 & 0 & 0 & 1 & 0 & 0 & 0 & 0 & 0 \\ 0 & 0 & 0 & 0 & T_v/\mu_v & 0 & 0 & 0 & 0 \\ 0 & 0 & 0 & 0 & 0 & T_v/\mu_v & 0 & 0 & 0 \\ 0 & 0 & 0 & 0 & 0 & 0 & T_v/\mu_v & 0 & 0 \\ 0 & 0 & 0 & 0 & 0 & 0 & 0 & T_h/\mu_h & 0 \\ 0 & 0 & 0 & 0 & 0 & 0 & 0 & 0 & T_h/\mu_h \end{bmatrix}. \tag{2.37}
$$

The wave structure of the system can be analyzed by the Jacobian matrix projected along an arbitrary vector, (n_x, n_y):

$$
\mathbf{PA}_n \equiv \mathbf{P}\left(\frac{\partial \mathbf{F}}{\partial \mathbf{U}} n_x + \frac{\partial \mathbf{G}}{\partial \mathbf{U}} n_y\right). \tag{2.38}
$$

Again, we split the Jacobian into the inviscid and viscous parts:

$$
\mathbf{PA}_n = \mathbf{PA}_n^i + \mathbf{PA}_n^v, \tag{2.39}
$$

where $\mathbf{A}_n^i$ and $\mathbf{A}_n^v$ are the projected Jacobians derived from the inviscid and viscous fluxes, respectively. The eigen-structure of the inviscid Jacobian is well known: the eigenvalues are

$$
\lambda_1^i = u_n - a, \quad \lambda_2^i = u_n, \quad \lambda_3^i = u_n, \quad \lambda_4^i = u_n + a, \quad \lambda_{5,6,7,8,9}^i = 0, \tag{2.40}
$$

where $u_n = un_x + vn_y$. The corresponding linearly independent right-eigenvectors are denoted by $\mathbf{r}_k^i$, $k = 1, 2, 3, \ldots, 9$. The first four eigenvectors represent the inviscid acoustic, shear, and entropy waves, constituting the inviscid subspaces. The other eigenvectors, $\mathbf{r}_k^i$, $k = 5, 6, 7, 8, 9$, are the vectors having 1 in the k-th component and 0 elsewhere. The viscous Jacobian has the following eigenvalues,

$$
\lambda_1^v = -a_{nv}, \quad \lambda_2^v = a_{nv}, \quad \lambda_3^v = -a_{mv}, \quad \lambda_4^v = a_{mv}, \quad \lambda_5^v = -a_h, \quad \lambda_6^v = a_h, \quad \lambda_{7,8,9}^v = 0, \tag{2.41}
$$

where

$$
a_{nv} = \sqrt{\frac{\nu_v}{T_v}}, \quad a_{mv} = \sqrt{\frac{3\nu_v}{4T_v}}, \quad a_h = \sqrt{\frac{\nu_h}{T_h}}. \tag{2.42}
$$

The speed, a_{nv}, is associated with the normal viscous stress; it is called the normal viscous wave. On the other hand, a_{mv} is associated with the shear viscous stress; it is called the shear viscous wave. As in one dimension, a_h is the speed of the heating wave. The corresponding linearly independent right-eigenvectors can be found and denoted by $\mathbf{r}_k^v$, $k = 1, 2, 3, \ldots, 9$. Thus, *the viscous part is a hyperbolic system by itself*, describing the isotropic normal/shear viscous and heating waves.

In both the inviscid and viscous parts, the corresponding left-eigenvectors denoted by $\boldsymbol{\ell}_k^i$ and $\boldsymbol{\ell}_k^v$, $k = 1, 2, 3, \ldots, 9$ can be found. Then, the full Jacobian can be expressed as a sum of 10 (not necessarily orthogonal) subspaces:

$$
\mathbf{PA} = \sum_{k=1}^{4} \lambda_k^i \mathbf{\Pi}_k^i + \sum_{k=1}^{6} \lambda_k^v \mathbf{\Pi}_k^v, \tag{2.43}
$$

where $\mathbf{\Pi}_k^i$ and $\mathbf{\Pi}_k^v$ are the pure inviscid and viscous projection matrices,

$$
\mathbf{\Pi}_k^i = \mathbf{r}_k^i \boldsymbol{\ell}_k^i, \quad \mathbf{\Pi}_k^v = \mathbf{r}_k^v \boldsymbol{\ell}_k^v. \tag{2.44}
$$

As in one dimension, the subspaces are orthogonal only within the inviscid and viscous parts, not orthogonal across them.

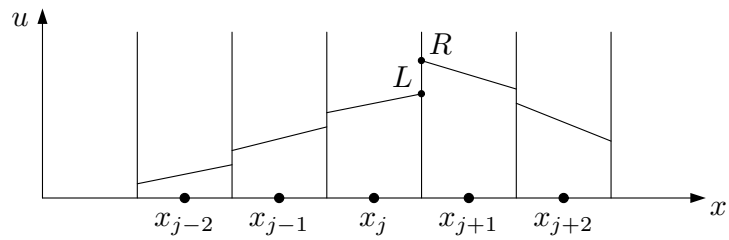

Figure 3.1. Piecewise linear data in one dimension.

3. Discretization

3.1. One Dimension

Consider a one-dimensional grid of N nodes with uniform spacing, h. The solution data are stored at the nodes denoted by x_j, $j = 1, 2, 3, \ldots, N$. Integrating the hyperbolic Navier-Stokes system over a dual cell, $I_j = [x_{j-1/2}, x_{j+1/2}]$, we obtain a standard semi-discrete finite-volume discretization:

$$\mathbf{P}_j^{-1} \frac{d\mathbf{U}_j}{dt} = -\frac{1}{h}\left[\mathbf{F}_{j+1/2} - \mathbf{F}_{j-1/2}\right] + \frac{1}{h}\int_{I_j} \mathbf{S}\, dx, \tag{3.1}$$

where $\mathbf{U}_j$ denotes the solution value at the node j, and $\mathbf{F}_{j+1/2}$ is the interface flux to be defined. To achieve second-order accuracy, we compute the solution gradients by the central-difference formula at each node, and reconstruct a piecewise linear solution within each dual volume as shown in Figure 3.1. Because the system is hyperbolic, we define the interface flux as an upwind flux of the form:

$$\mathbf{F}_{j+1/2} \quad = \quad \frac{1}{2}\left[\mathbf{F}_R + \mathbf{F}_L\right] - \frac{1}{2}\mathbf{P}^{-1}\left|\mathbf{PA}\right| \Delta\mathbf{U}, \tag{3.2}$$

where $\Delta\mathbf{U} = \mathbf{U}_R - \mathbf{U}_L$, $\mathbf{U}_R$ and $\mathbf{U}_L$ denote the extrapolated solution values at the interface, and $\mathbf{F}_R$ and $\mathbf{F}_L$ are the physical fluxes evaluated by these interface values. Note that the dissipation term has been constructed following the well-known procedure in the local preconditioning technique [10]. The evaluation of the absolute Jacobian, $|\mathbf{PA}|$, requires the complete eigen-structure of the full Jacobian that is not known at the moment. Here, we take the following approximate approach:

$$|\mathbf{PA}| \approx \sum_{k=1}^{3} |\lambda_k^i| \mathbf{\Pi}_k^i + \sum_{k=1}^{4} |\lambda_k^v| \mathbf{\Pi}_k^v. \tag{3.3}$$

This is a crude but reasonably simple approximation. It is possible and perhaps more sensible to weight them by the Reynolds number as suggested in Ref. [2]. The precise form and the effect of weighting is a subject of future work. The interface quantities necessary to evaluate the dissipation matrix are computed by the Roe-averages [11] in the inviscid part and by the arithmetic averages in the viscous part. In the inviscid limit, the resulting numerical flux will, therefore, reduce to the Roe flux [11]. The viscous part of the dissipation term can be simplified, and here it is implemented as a single vector. We emphasize that this is an upwind scheme for the hyperbolic Navier-Stokes system; *it is upwind for all Reynolds numbers.* To integrate in time, we employ the forward Euler explicit scheme with the time step restricted by

$$\Delta t = \mathrm{CFL} \frac{h}{\max(|u| + a + a_h)_j}, \tag{3.4}$$

where CFL is the Courant-Friedrichs-Lewy number less than or equal to 1, and the denominator is the maximum wave speed approximated as the sum of the maximum inviscid wave speed and the maximum viscous wave speed ($a_v < a_h$ for air). Observe that the time step is $O(h)$, not $O(h^2)$ which is typical in traditional Navier-Stokes schemes. It should be emphasized here that this $O(h)$ time step is not a particular feature of the finite-volume scheme above; it is an intrinsic feature of numerical schemes solving the hyperbolic Navier-Stokes system.

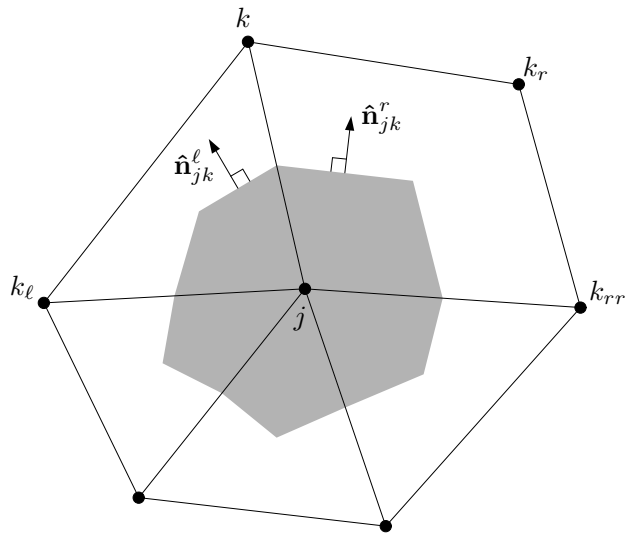

Figure 3.2. Dual control volume for node-centered finite-volume schemes with unit normals associated with an edge, $\{j, k\}$.

3.2. Two Dimensions

Given a computational grid composed of quadrilaterals and/or triangles, we store the solution data at nodes, and discretize the hyperbolic Navier-Stokes system by the edge-based finite-volume method:

$$\mathbf{P}_j^{-1}\frac{d\mathbf{U}_j}{dt} = -\frac{1}{V_j}\sum_{k\in\{K_j\}}\mathbf{\Phi}_{jk}A_{jk} + \frac{1}{V_j}\int_{\Omega_j}\mathbf{S}\,dV, \tag{3.5}$$

where $\mathbf{U}_j$ is the solution vector at the node j, V_j is the median dual volume, $\{K_j\}$ is a set of neighbors of the node j, $\mathbf{\Phi}_{jk}$ is a numerical flux along the directed area vector (see Figure 3.2),

$$\mathbf{n}_{jk} = \mathbf{n}^\ell_{jk} + \mathbf{n}^r_{jk}, \tag{3.6}$$

defined at the midpoint of the edge, and A_{jk} is the magnitude of the directed area vector (i.e., $A_{jk} = |\mathbf{n}_{jk}|$). For second-order accuracy, we compute the solution gradients by the unweighted least-squares method at nodes, and reconstruct a linear solution within each dual control volume. On the boundary, a suitable boundary flux is applied with the linearity-preserving quadrature formulas [3,12] (see Appendices of Ref. [3] for a comprehensive list of linearity-preserving quadrature formulas in both two and three dimensions). We define the numerical flux as an upwind flux of the form:

$$\mathbf{\Phi}_{jk} = \frac{1}{2}\left[\mathbf{H}_{jk}\left(\mathbf{U}_R\right) + \mathbf{H}_{jk}\left(\mathbf{U}_L\right)\right] - \frac{1}{2}\mathbf{P}^{-1}\left|\mathbf{P}\mathbf{A}_n\right|\Delta\mathbf{U}, \tag{3.7}$$

where $\Delta\mathbf{U} = \mathbf{U}_R - \mathbf{U}_L$, $\mathbf{U}_R$ and $\mathbf{U}_L$ are the extrapolated solution vectors at the midpoint of the edge, $\{j, k\}$, $\mathbf{H}_{jk}$ is the physical flux projected along the directed area vector,

$$\mathbf{H}_{jk} = [\mathbf{F}, \mathbf{G}]\cdot\hat{\mathbf{n}}_{jk}, \quad \hat{\mathbf{n}}_{jk} = \frac{\mathbf{n}_{jk}}{|\mathbf{n}_{jk}|}, \tag{3.8}$$

and $\mathbf{A}_n = \partial\mathbf{H}_{jk}/\partial\mathbf{U}$. The dissipation matrix is again computed by the simple approximation:

$$|\mathbf{P}\mathbf{A}_n| \approx \sum_{k=1}^{4}|\lambda^i_k|\mathbf{\Pi}^i_k + \sum_{k=1}^{6}|\lambda^v_k|\mathbf{\Pi}^v_k. \tag{3.9}$$

The interface quantities are computed similarly as in one dimension; and thus the resulting numerical flux will reduce to the Roe flux in the inviscid limit. Also, we simplified the viscous part of the dissipation term and implemented it as a single vector. Note that the resulting numerical flux is upwind for *all Reynolds numbers*. The

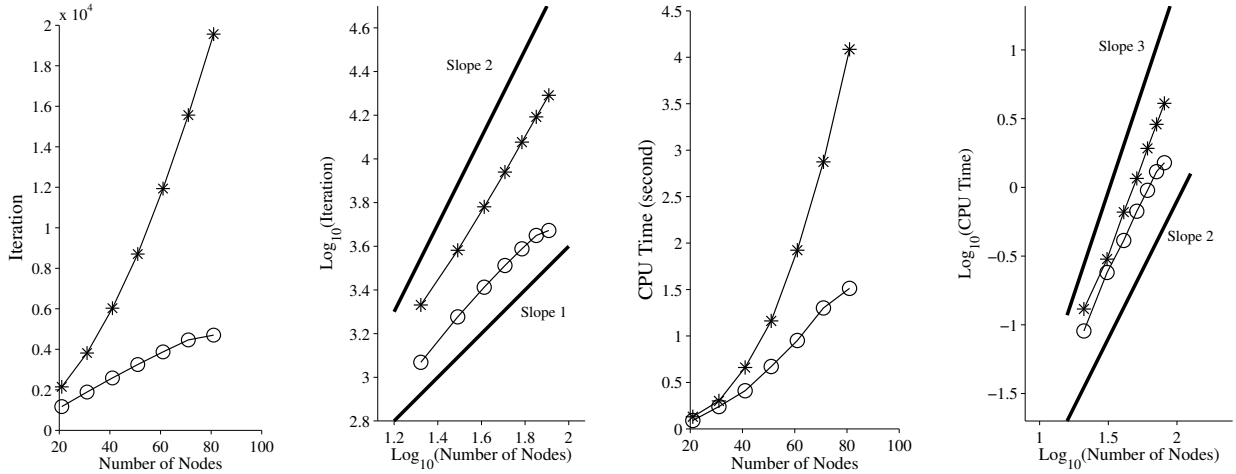

(a) Iteration vs. N (b) Log-log plot of (a). (c) CPU time vs. N. (d) Log-log plot of (c).

Figure 3.3. Convergence results for the one-dimensional problem. Stars: the traditional scheme. Circles: the hyperbolic scheme.

semi-discrete equation (3.5) is then integrated in time by the forward-Euler time-stepping scheme. The global time-step, Δt, is defined as the minimum of the local time-step, Δt_j, restricted by the local CFL condition:

$$\Delta t_j = \text{CFL}\frac{2V_j}{\sum_{k\in\{K_j\}} (|u_n| + a + a_h)_j A_{jk}}, \quad \text{CFL} \leq 1. \tag{3.10}$$

Again, the time step is $O(h)$, not $O(h^2)$; it is an intrinsic property of numerical schemes solving the hyperbolic Navier-Stokes system.

4. Results

Preliminary results are available for a viscous shock-structure problem whose exact solution can be obtained by numerically solving a pair of ordinary differential equations for the velocity and the temperature [13]. The program used to generate the exact solution in this study can be downloaded at `http://www.cfdbooks.com/cfdcodes.html`. In all computations, we take $M_\infty = 3.5$, $Pr = 3/4$, $\gamma = 1.4$, $Re_\infty = 25$, and $T_\infty = 400$ [k].

4.1. One-Dimensional Problem

We use the exact solution as the initial solution, and integrate the hyperbolic Navier-Stokes system toward the steady state with CFL= 0.99. The domain is taken as $x = [-1, 1]$. All grids are uniformly spaced with 21, 31, 41, 51, 61, 71, 81 nodes. To fix the shock location, we keep the exact pressure at $x = 0.5$ for all grids. On the left and right boundaries, the flux is computed by the numerical flux with the left and right states given by the exact solutions, respectively. The steady state is taken as reached when the divided residual is reduced by six orders of magnitude in the L_1 norm. The hyperbolic Navier-Stokes scheme is compared with a traditional Navier-Stokes scheme based on the Roe flux for the inviscid term and the central-difference scheme for the viscous term.

Figure 3.3 shows the convergence results for the hyperbolic Navier-Stokes scheme and the traditional Navier-Stokes scheme. As seen from Figures 3(a) and 3(b), the number of iterations for the traditional schemes shows a quadratic increase with the number of nodes. On the other hand, the number of iterations for the hyperbolic Navier-Stokes scheme increases linearly with the number of nodes. These behaviors agree with the results in Ref. [2]. This tremendous speed-up is carried over to the CPU time required to reach the steady state as shown in Figure 3(c). Every iteration requires $O(N)$ work, and therefore we expect that the CPU time increases as $O(N^3)$ and $O(N^2)$ for the traditional and hyperbolic schemes, respectively. These estimates are confirmed by Figure 3(d). The hyperbolic scheme is, therefore, faster than the traditional scheme despite the fact that it

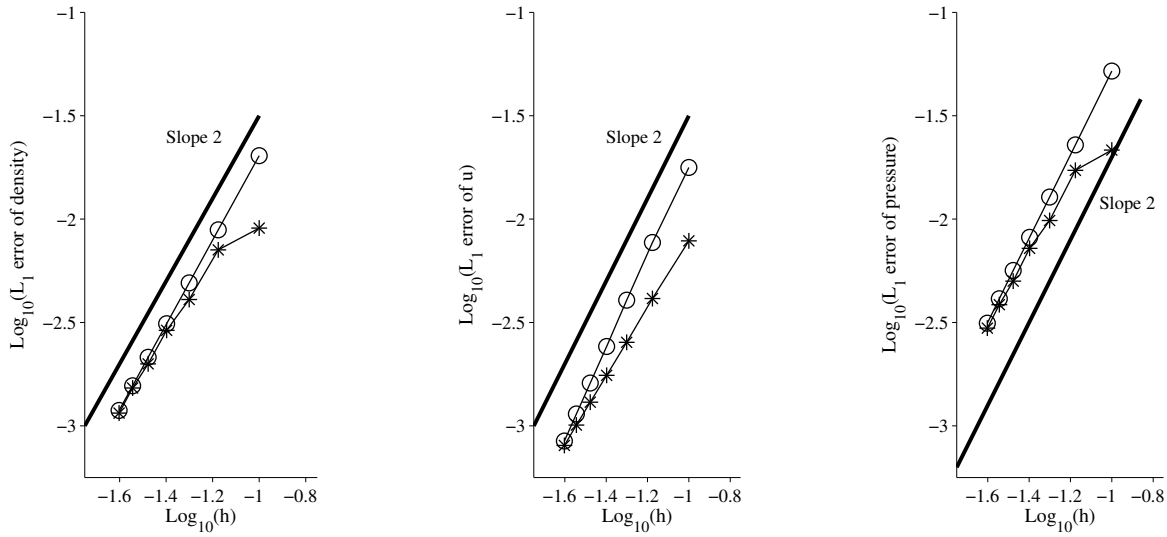

(a) L_1 error of ρ. (b) L_1 error of u. (c) L_1 error of p.

Figure 4.1. Error convergence results for the main variables in the one-dimensional problem. Stars: the traditional scheme. Circles: the hyperbolic scheme.

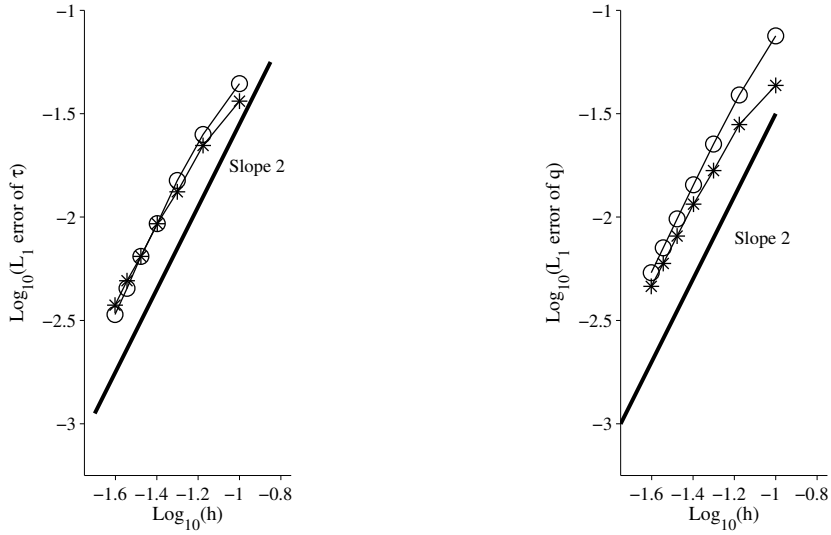

(a) L_1 error of τ. (b) L_1 error of q.

Figure 4.2. Error convergence results for the viscous stress and the heat flux in the one-dimensional problem. Stars: the traditional scheme. Circles: the hyperbolic scheme.

carries more unknowns and solves equations for them. The speed-up factor is $O(1/h)$ in both iterations and CPU time; the factor increases with the problem size. A clever programming or code optimization may bring the CPU time further down for the traditional scheme, but it will be difficult, if not impossible, to change the cubic increase. The hyperbolic scheme will dominate performance eventually as the number of nodes increases.

Error convergence results are given in Figures 4.1 and 4.2. For the traditional scheme, the viscous stress and the heat flux were computed at the end of the iterations by the central-difference formula. In this case, on uniform grids, we expect second-order accuracy in all variables for both schemes. These figures show, indeed, that both schemes are second-order accurate in all variables. Superior accuracy in the viscous stress and the

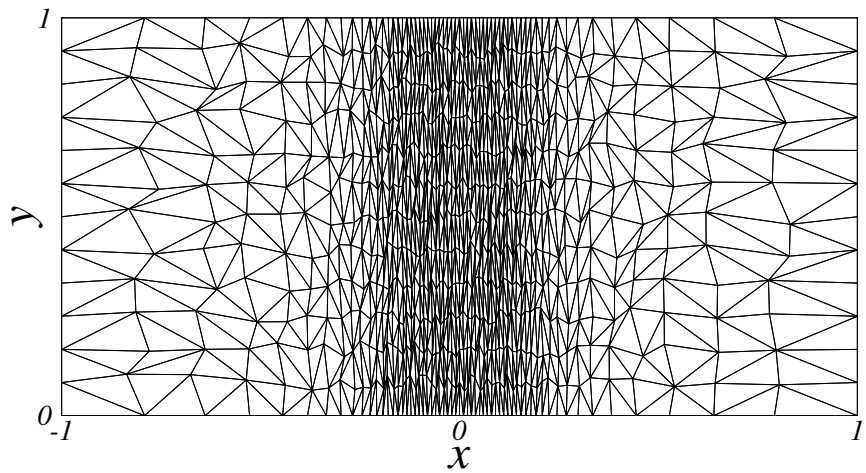

Figure 4.3. Irregular triangular grid for the viscous shock-structure problem (793 nodes).

heat flux by the hyperbolic scheme is observed on unstructured grids, which we show for a two-dimensional problem.

4.2. Two-Dimensional Problem

We consider the one-dimensional viscous shock-structure problem in a two-dimensional rectangular domain. Results are available for irregular triangular grids generated from 21x5, 41x9, 61x13, 81x17, 101x21 regular grids by random perturbation, random diagonal splitting, and stretching. In each grid, the nodes are clustered over the viscous shock as shown in Figure 4.3. Again, the exact solution is used as the initial solution. Also, a similar internal pressure condition and boundary conditions are applied as in one dimension. Time integration is performed with CFL= 0.99 until the divided residual is reduced by six orders of magnitude in the L_1 norm. The hyperbolic Navier-Stokes scheme is compared with a traditional Navier-Stokes scheme based on the Roe flux for the inviscid term and the face-tangent average-least-squares scheme for the viscous term [3, 4].

Figure 4.4 shows the convergence results for the hyperbolic Navier-Stokes scheme and the traditional Navier-Stokes scheme. As clearly seen in Figure 4(a), the traditional scheme takes orders of magnitude larger number of iterations to reach the steady state than the hyperbolic scheme. As predicted in Ref. [2] and confirmed by Figure 4(b), it increases linearly with the total number of nodes, denoted by N, for the traditional scheme while it is proportional to the square root of the number of nodes for the hyperbolic Navier-Stokes scheme. As demonstrated in Figure 4(c), the speed-up in iterations does overwhelm the additional cost of carrying more unknowns and solving the equations for them. Every iteration requires $O(N)$ work, and therefore we expect that the CPU time increases as $O(N^2)$ and $O(N^{1.5})$ for the traditional and hyperbolic schemes, respectively. These estimates are confirmed by Figure 4(d). Again, the speed-up is $O(1/h)$ in both iterations and CPU time. Note again that the speed-up factor grows with the number of nodes. The hyperbolic scheme gets faster and faster than the traditional scheme for larger-scale problems.

Error convergence results are given in Figures 4.5 and 4.6. For the traditional scheme, the viscous stress and the heat flux were computed once at the end of the iterations by the unweighted least-squares reconstruction. Figure 4.5 shows that both schemes are second-order accurate in the main flow variables. The traditional scheme has some irregularity in the error convergence. It is considered as a result of the mesh irregularity; we observed a uniform second order convergence for different sets of grids. Figure 4.6 shows the error convergence in the viscous stresses and the heat fluxes (τ_{yy} is equivalent to τ_{xx}, and thus the result is not shown). As expected, the hyperbolic scheme achieved second-order accuracy in these quantities. The reconstructed values for the traditional scheme are only first-order accurate. This difference in the order of error convergence implies orders of magnitude smaller errors in further grid refinement. We emphasize that this superior accuracy in the viscous stresses and the heat fluxes comes with the $O(1/h)$ faster iterative convergence. Even if second-order accuracy is achieved by high-order or implicit reconstruction for the traditional scheme, it remains extremely slower than the hyperbolic scheme.

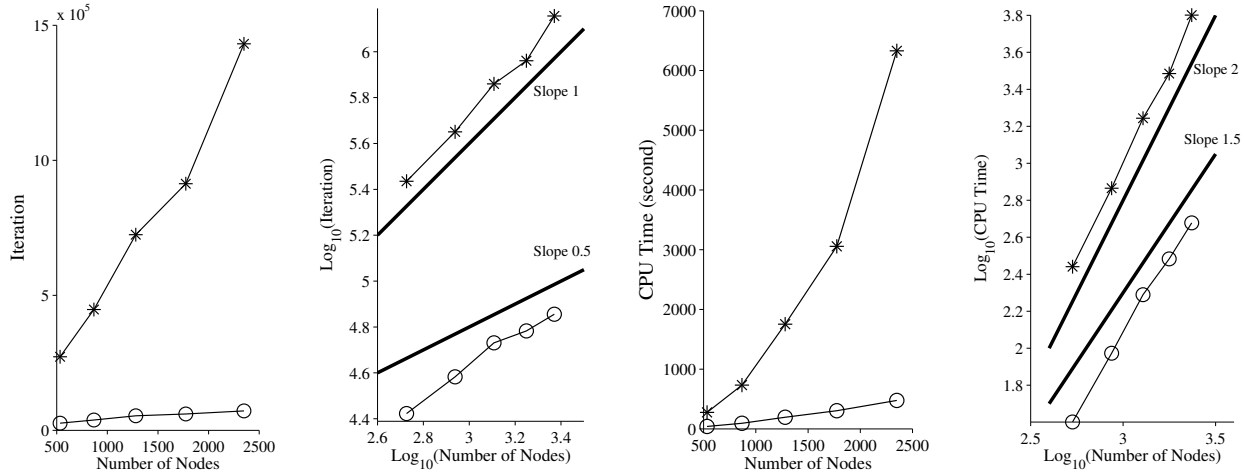

(a) Iteration vs. N (b) Log-log plot of (a). (c) CPU time vs. N. (d) Log-log plot of (c).

Figure 4.4. Convergence results for the two-dimensional problem. Stars: the traditional scheme. Circles: the hyperbolic scheme.

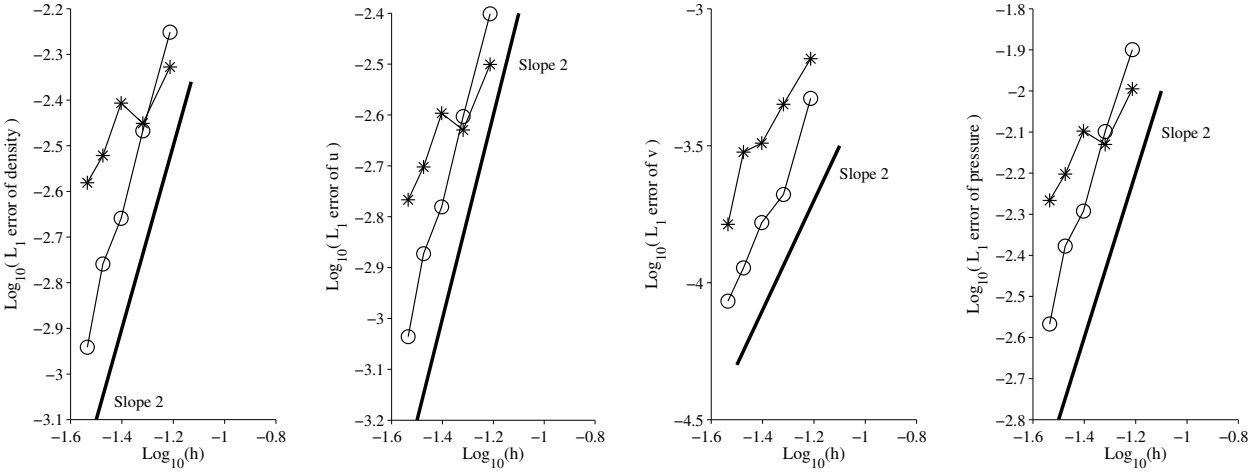

(a) L_1 error of ρ. (b) L_1 error of u. (c) L_1 error of v. (d) L_1 error of p.

Figure 4.5. Error convergence results for the main variables in the two-dimensional problem. Stars: the traditional scheme. Circles: the hyperbolic scheme.

5. Concluding Remarks and Future Developments

In this paper, we have introduced a first-order hyperbolic Navier-Stokes system to compute the steady state solution of the compressible Navier-Stokes equations. A finite-volume scheme has been constructed for the hyperbolic system based on an upwind flux. Preliminary results demonstrated the advantages of the resulting Navier-Stokes code over traditional Navier-Stokes codes: the $O(1/h)$ speed-up by the explicit time-stepping scheme and the second-order accuracy of the viscous stresses and the heat fluxes on fully irregular unstructured grids.

For a simple and systematic discretization, we have introduced a preconditioned conservative form of the hyperbolic Navier-Stokes system. This particular approach greatly simplifies the analysis of the wave structure of the system by avoiding complications arising from the nonlinearity. It also paves the way for further improvements by setting a stage for the local preconditioning technique to ensure the accuracy in the low-Mach number limit as well as to accelerate the convergence to the steady state [14]. If the full eigen-structure were available

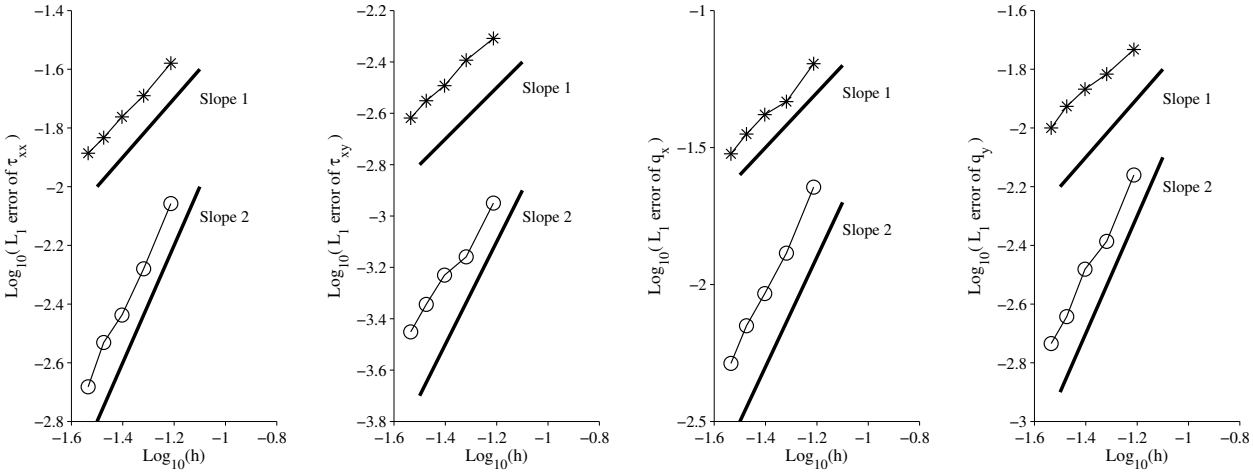

(a) L_1 error of τ_{xx}. (b) L_1 error of τ_{xy}. (c) L_1 error of q_x. (d) L_1 error of q_y.

Figure 4.6. Error convergence results for the viscous stresses and the heat fluxes in the two-dimensional problem. Stars: the traditional scheme. Circles: the hyperbolic scheme.

for the hyperbolic system in the steady form, the optimal local preconditioning matrix could be constructed for the whole system in one and two dimensions [14]. This preconditioned-form approach is a general approach applicable to other nonlinear equations. It makes the proposed method available to a wide range of practical applications. Also, we have introduced an approximate evaluation of the upwind dissipation matrix: the full absolute Jacobian is approximated by a sum of the inviscid and viscous absolute Jacobians. This approximate approach simplifies the construction of the interface flux for the hyperbolic Navier-Stokes system. Although the approach has been found successful for the problem considered here, it may be more sensible to weight them by the Reynolds number as suggested in Ref. [2]. Yet, we may simply view it as a sum of the Roe inviscid flux and the upwind viscous flux, and explore other choices for each flux. For example, we can employ a more robust inviscid flux such as the Rotated-RHLL flux [15] for applications involving strong shocks.

For flows with shock waves, a mechanism to prevent oscillations such as a limiter needs to be incorporated, perhaps, not only for the main flow variables but also for the extra variables. It can be considered as introducing a means to control the nonlinear stability such as the positivity of the viscous discretization. Positivity is considered as a very important property for the viscous discretization, but it remains difficult to devise a positive viscous discretization on general unstructured grids. In the first-order hyperbolic system method, if we have a positive scheme for the inviscid term, we almost immediately have a positive scheme for the viscous term. The development of shock-capturing hyperbolic Naiver-Stokes schemes is underway. In practical applications, the computational grid is typically highly-stretched for resolving viscous layers. For such grids, it would be desired to have implicit time-stepping schemes available. In this case, the residual Jacobian, which needs to be inverted at every time step, has an $O(h)$ times smaller condition number, and thus we expect $O(1/h)$ faster iterative convergence. The development of implicit time-stepping schemes is a very important subject of future work. Eventually, we will extend the method to time-accurate simulations by employing the dual-time stepping technique where the Navier-Stokes code arising from the proposed method can be used in the inner iteration. A rapid convergence is expected over each physical time step. It should be noted that the first-order hyperbolic system for the Navier-Stokes equations is by no means unique. There are many other possible choices. For example, an alternative system can be constructed such that it leads to not only accurate viscous stresses and heat fluxes but also accurate vorticity on unstructured grids. The development of such alternative systems is currently underway.

The first-order hyperbolic system method is a general method applicable to various partial differential equations involving second and higher order derivatives. As shown in Ref. [1], $O(1/h)$ times faster iterative methods can be constructed for the Laplace/Poisson type equations with accurate solution gradients simultaneously computed. Applications of the resulting fast elliptic solvers include the elliptic grid generation/adaptation, the Poisson equation for the pressure in the incompressible Navier-Stokes equations, etc. In Ref. [2], the method was extended to the advection-diffusion equation, and in particular a uniform iterative convergence over a wide range

of Reynolds numbers was demonstrated for boundary-layer type problems on stretched grids. The resulting hyperbolic advection-diffusion scheme can be readily applied, for example, to scalar turbulence model equations. Application to higher-order derivative terms is also possible: construct an extended first-order hyperbolic system and solve it by an upwind scheme. That is, partial differential equations of arbitrary order can be discretized by methods for hyperbolic systems, and it leads to orders of magnitude more efficient and accurate solvers. Finally, the method has been extended to nonlinear systems in this paper. Opportunities for practical applications are now wide open: incompressible Navier-Stokes equations, thermal flow and heat transfer phenomena in nuclear applications, resistive magneto-hydrodynamic simulations, ground-water simulations in hydro-geology, chemical diffusion, and so on. The impact of the proposed method on the future CFD development is expected to grow larger as the grid size gets larger and the geometry gets more complex. This paper has just opened the door to the next generation of CFD codes. It is only the beginning.

Acknowledgments

The author would like to thank Charles C. Swanson (NASA Langley Research Center) for his valuable comments. This work was partly supported by the NASA Fundamental Aeronautics Program through NASA Research Announcement Contract NNL07AA23C.

References

[1]Nishikawa, H., "A First-Order System Approach for Diffusion Equation. I: Second-Order Residual-Distribution Schemes," *Journal of Computational Physics*, Vol. 227, 2007, pp. 315–352.

[2]Nishikawa, H., "A First-Order System Approach for Diffusion Equation. II: Unification of Advection and Diffusion," *Journal of Computational Physics*, Vol. 229, 2010, pp. 3989–4016.

[3]Nishikawa, H., "Beyond Interface Gradient: A General Principle for Constructing Diffusion Schemes," *40th AIAA Fluid Dynamics Conference and Exhibit*, AIAA Paper 2010-5093, Chicago, 2010.

[4]Nishikawa, H., "Robust and Accurate Viscous Discretization via Upwind Schemes, I: Basic Principle," *Computers and Fluids*, 2011, in press.

[5]Girault, V. and Raviart, P. A., "An analysis of a mixed finite element method for the Navier-Stokes equations," *Numerische Mathematik*, Vol. 33, 1979, pp. 235–271.

[6]Heys, J., Lee, E., Manteuffel, T., and McCormick, S., "An alternative least-squares formulation of the Navier-Stokes equations with improved mass conservation," *Journal of Computational Physics*, Vol. 226, 2008, pp. 944–1006.

[7]Jiang, B.-N., *The Least-Squares Finite Element Method*, Springer, 1998.

[8]Gnoffo, P. A., "Multi-Dimensional, Inviscid Flux Reconstruction for Simulation of Hypersonic Heating on Tetrahedral Grids," AIAA Paper 2009-599, 2009.

[9]Kitamura, K., Nakamura, Y., and Shima, E., "An Evaluation of Euler Fluxes II: Hypersonic Surface Heating Computation," *38th AIAA Fluid Dynamics Conference and Exhibit*, AIAA Paper 2009-3648, Seattle, 2008.

[10]van Leer, B., Lee, W.-T., and Roe, P. L., "Characteristic Time-Stepping or Local Preconditioning of the Euler Equations," *10th AIAA Computational Fluid Dynamics Conference*, AIAA Paper 91-1552, Hawaii, 1991.

[11]Roe, P. L., "Approximate Riemann Solvers, Parameter Vectors, and Difference Schemes," *Journal of Computational Physics*, Vol. 43, 1981, pp. 357–372.

[12]Diskin, B. and Thomas, J. L., "Accuracy Analysis for Mixed-Element Finite-Volume Discretization Schemes," *NIA Report No. 2007-08*, 2007.

[13]Xu, K., "A Gas-Kinetic BGK Scheme for the Navier-Stokes Equations and Its Connection with Artificial Dissipation and Godunov Method," *Journal of Computational Physics*, Vol. 171, 2001, pp. 289–335.

[14]Nishikawa, H., Roe, P., Suzuki, Y., and van Leer, B., "A General Theory of Local Preconditioning and Its Application to the 2D Ideal MHD Equations," *16th AIAA Computational Fluid Dynamics Conference*, AIAA Paper 2003-3704, Orlando, 2003.

[15]Nishikawa, H. and Kitamura, K., "Very Simple, Carbuncle-Free, Boundary-Layer Resolving, Rotated-Hybrid Riemann Solvers," *Journal of Computational Physics*, Vol. 227, 2007, pp. 2560–2581.